Research Experience for Undergraduates in Chemistry.
Final Report.
Summer 1992

Computational Studies of Proton Tranfer Along Hydroxyl Chains.

Félix Fernández-Alonso.
Hamilton College.
Clinton, NY 13323

Performed under the supervision of Dr. Carl Trindle.

Table of Contents

1. Introduction.

1.1 Background and brief description of the project.

The hydrogen bond has been a very active area of research and speculation since Latimer and Rodebush proposed its existence in 1920 [1]. Today, hydrogen bonding is known to play a crucial role in many important phenomena such as protein conformation or proton transfer mechanisms in biological systems.

In general, hydrogen bonds are recognized to exist between a hydrogen bound to a electronegative atom and a second electronegative atom in the near vicinity (1.8-2.0 Å). This useful but simple conception has allowed the recognition of hydrogen bonds in many different systems. However, this descriptive picture of a hydrogen bond is of limited help to the theoretician, interested in analyzing the intrinsic nature of the interaction.

Our goal is to describe hydrogen bonds in small organic systems, using molecular mechanics, semiempirical and *ab initio* methods and to analyze the proton transfer processes that could take place in chains of hydrogen bonds. A model system, suggested by Professor Glenn McGarvey, is shown below. We plan to trace the passage of a proton from a neighboring H_3O^+ to the terminal hydroxyl of the tricyclic system, and down the hydroxyl chain.

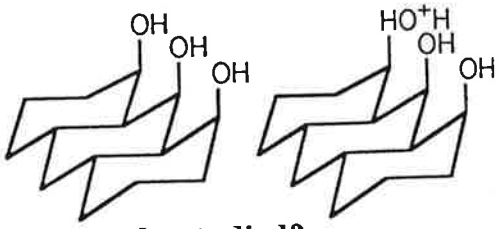

1.2 How are hydrogen bonds studied?

1.2.1 Experimental Methods

The most-widely used techniques for the study of hydrogen bonds are: X-ray diffraction, neutron scattering, infrared and Raman vibrational spectroscopy, nuclear magnetic resonance and microwave spectroscopy [2]. Each of these techniques has its pros and cons, which we list in the table.

METHOD	Strength	Drawback
X-ray crystallography	Unambiguous location of heavy atoms	Imprecise location of hydrogen atoms
Neutron diffraction	Unambiguous location of Hydrogen atoms	Cost, inconvenience
Infrared and Raman vibrational spectroscopy	Hints at bond strengths, strength of coupling, and overall symmetry	Incomplete data; low-frequency modes often inaccessible
Nuclear magnetic resonance	Gives information on the proton environment	
Microwave spectroscopy	Can estimate molecular geometries with high accuracy	Requires volatile species with permanent dipole

Schuster et al. [3] have summarized the structural and spectroscopic features associated with hydrogen bonds, of form AH..B.

- The distances between the atoms A and B of the two functional groups (AH···B) involved in H-bonds are substantially smaller than the sum of the A-H and B van der Waals' radii.
- The AH bond length is increased upon H-bond formation.
- The H-bond stretching modes are shifted towards lower frequencies on H-bond formation.
- The polarities of AH bonds increase upon H-bond formation, usually leading to larger dipole moments. Furthermore, also the significantly enhanced IR intensities indicate an increase in the dipole moment on H-bond formation.
- NMR chemical shifts of protons in H-bonds are substantially smaller than those observed in the corresponding isolated molecules. This is due to reduced electron densities at protons involved in H-bonding.

1.2.2 Theoretical (computational) Methods

Three computational methods may be applied to the problem of characterizing hydrogen-bonding systems.

- Molecular Mechanics methods (hundred of atoms)

These methods represent the molecular potential by classical models, parametrized to reproduce a variety of structural properties. A number of alternative force fields are available, among them Allinger's MM1, MM2 and MM3, Kollman's AMBER, Tripos Corporation's ALCHEMY III, and Karplus' CHARMM. These calculations are cheap and very fast but not always reliable or conducive of insight. Molecular mechanics is probably the method of choice in early stages of description and study of large molecular systems. It produces descriptions of molecules which generally agree with our chemical intuition, but cannot deal with systems with unconventional (*i.e.*, nonlocal or strained) bonding.

- Semiempirical methods (scores of atoms)

These models are derived from the methods of molecular quantum mechanics, and are all based on the Roothaan SCF-MO formalism. These methods, in rough order of complexity, computational demands, and reliability, go under the names Extended Hückel, CNDO/INDO, MNDO. The most recently developed parametrization within the MNDO family is called PM3. Specially parametrized methods have been developed for the description of magnetic resonance, electronic spectra, and the structure of organometallics. In favorable cases these methods yield results comparable in accuracy with *ab initio* methods, but fail unpredictably.

- *Ab Initio* methods (tens of atoms)

  These methods, developed for a broad chemical clientele by Pople and collaborators, are in principle not limited in accuracy, and can be systematically improved. Calculations of high accuracy are very costly and demanding of computer resources, and are limited to small systems. However the scope of these calculations advances as rapidly as computer power increases.

On theoretical grounds it is much harder to define or list a series of characteristics typical of hydrogen bonds. The two quotations given below illustrate this controversy.

- Electrostatic view: 'An AX...HYB is held together by a H-bond if the electrostatic potential surrounding X is negative, H is positive, and the X, H and Y are approximately collinear (...) Intramolecular H bonds pose a problem with the above, as do certain crystal H-bonds which appear to be reasonably strong despite their linearity' [4].

- Covalent view: 'The H-bond is viewed as an electron donor-acceptor complex in which a pair of electrons from the HOMO of the Lewis Base is donated to the LUMO of the Lewis acid' [5]

Definitely, there is still a lot to explain and investigate about the nature of H-bonds.

2. The Project: Computational Studies of Proton Tranfer Along Hydroxyl Chains.

2.1 Computational Methods and Implementation.

All calculations have been performed in the CAChe™ System and SPARTAN, available in a Personal Iris 4D/35 workstation.

Molecular mechanics, using Allinger's MM2 force field, has been used as the first tool when a new system had to be analyzed. Semiempirical molecular orbital methods were also available. Three possibilities were available to us, namely Extended Hückel, ZINDO (Zender's INDO program) and MOPAC (Molecular Orbital Package). Generally, MNDO PM3, included in MOPAC, was used after a molecular mechanics study of the system. Data from these calculations included the heat of formation, density matrix, Mulliken populations, geometric parameters (bond distances, angles, torsion angles, etc) and vibrational information (reduced masses, transition dipole moments, frequencies, etc).

Finally, the recent acquisition of SPARTAN allowed us to perform *ab initio* calculations for small (i.e. first-row hydride dimers, malonaldehyde) as well as large systems (cyclohexanol, bicyclic diols) at different levels of theory (STO-3G, 3-21G and 3-21G*).

2.2 Results and Discussion.

2.2.1 Calibration and Evaluation of the Accuracy of Approximate Theoretical Methods

2.2.1.1 Energy.

We tested the consistency of the description of hydrogen bonds provided by Allinger's MM2 force field and MNDO PM3 semiempirical model by calculating the optimum geometries and energies of nine different dimers involving water, hydrogen fluoride and ammonia. The data values calculated by each method are contrasted with those obtained from *ab initio* and experimental studies [6]. Both MM and MNDO generally underestimate the hydrogen bonding energy. Exceptions to this rule all involve HF. Excluding fluorine-bearing species from the comparisons improves the correlation considerably, as is shown in figures 1 and 2. Fluorine is a persistently difficult atom for computational methods; i.e. the stability of diatomic fluorine relative to atomic fluorine is not predicted by an *ab initio* SCF calculation in a small basis. In view of the fact that our proton transfer chains do not involve fluorine, we are not ready to discard these approximate methods.

Dimer	H-Bond Energy (Kcal/Mole)	
	Exp.	MM
HF-HF	4.60	0.14
Water-Water	5.30	3.26
Ammonia-Ammonia	2.70	1.28
HF(A)-Water(D)	3.00	1.08
HF(D)-Water(A)	9.40	0.40
HF(A)-Ammonia(D)	1.30	0.35
HF(D)-Ammonia(A)	11.70	0.14
Water(A)-Ammonia(D)	2.30	4.84
Water(D)-Ammonia(A)	5.80	3.76

Table 1. Experimental [7] versus MM H-bond energies. 'A' denotes proton acceptor while 'D' donor.

Fig. 1 MM vs. Literature H-Bond Energies

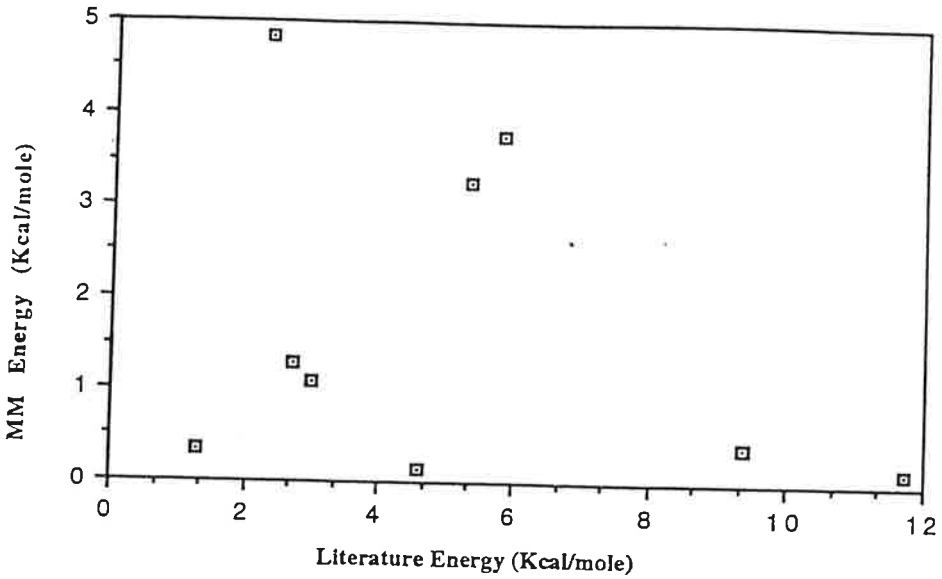

The scatter in this plot (figure 1) suggests that a systematic description of relative H-bond strengths is not provided by MM2. But if the problematic HF systems are dropped (figure 2), a correlation between MM and observed hydrogen bonding interactions is discernable.

Fig. 2 MM vs. Literature H-Bond Energies. Those dimers containing HF(D) have been removed.

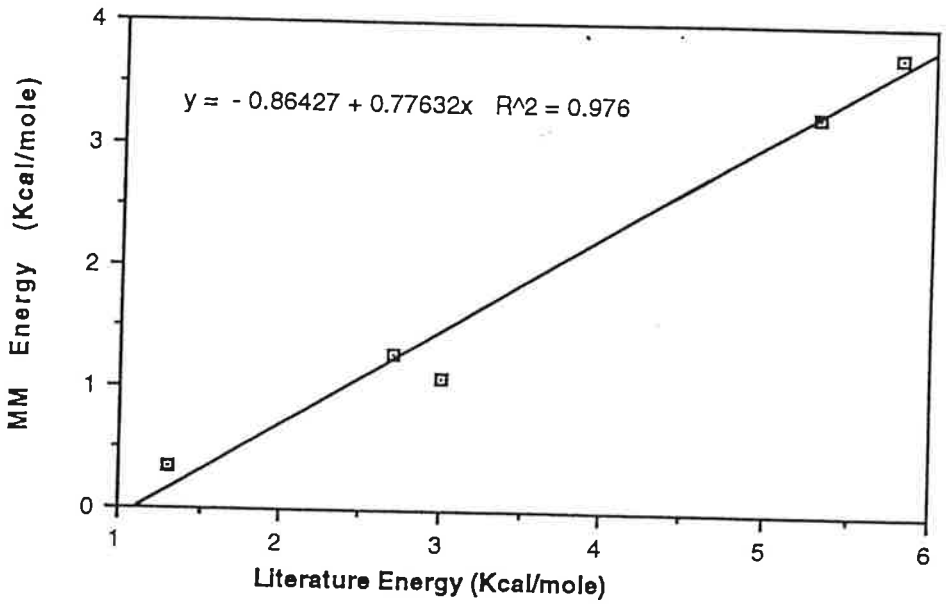

We consider next the MNDO-PM3 results. Once again, pair interaction energies are badly scattered, but removal of pairs involving HF produces a definite if rough correlation between computed and experimental estimates of the hydrogen bonding energy.

Dimer	H-Bond Energy (Kcal/Mole)	
	Experimental	MNDO-PM3
HF-HF	4.6	6.08
Water-Water	5.3	3.29
Ammonia-Ammonia	2.7	0.36
HF(A)-Water(D)	3	3.62
HF(D)-Water(A)	9.4	5.32
HF(A)-Ammonia(D)	1.3	1.17
HF(D)-Ammonia(A)	11.7	5.90
Water(A)-Ammonia(D)	2.3	0.64
Water(D)-Ammonia(A)	5.8	1.40

Table 2. Experimental [8] versus MNDO PM3 H-bond energies. Again, 'A' denotes proton acceptor while 'D' donor.

Fig. 3 MNDO-PM3 vs. Literature H-Bond Energies

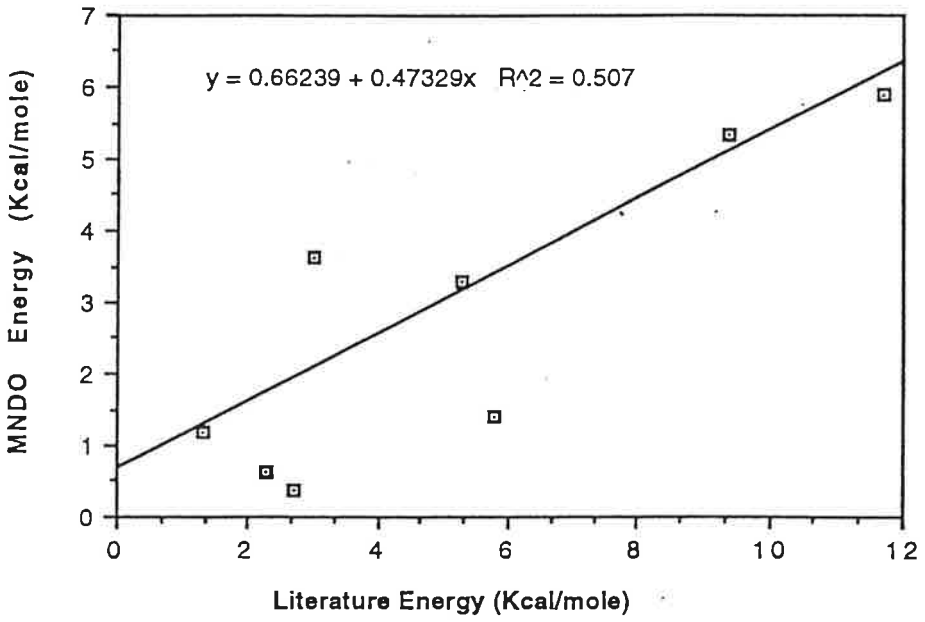

Fig. 4 MNDO-PM3 vs. Literature H-Bond Energies. Dimers involving HF(A) have been neglected.

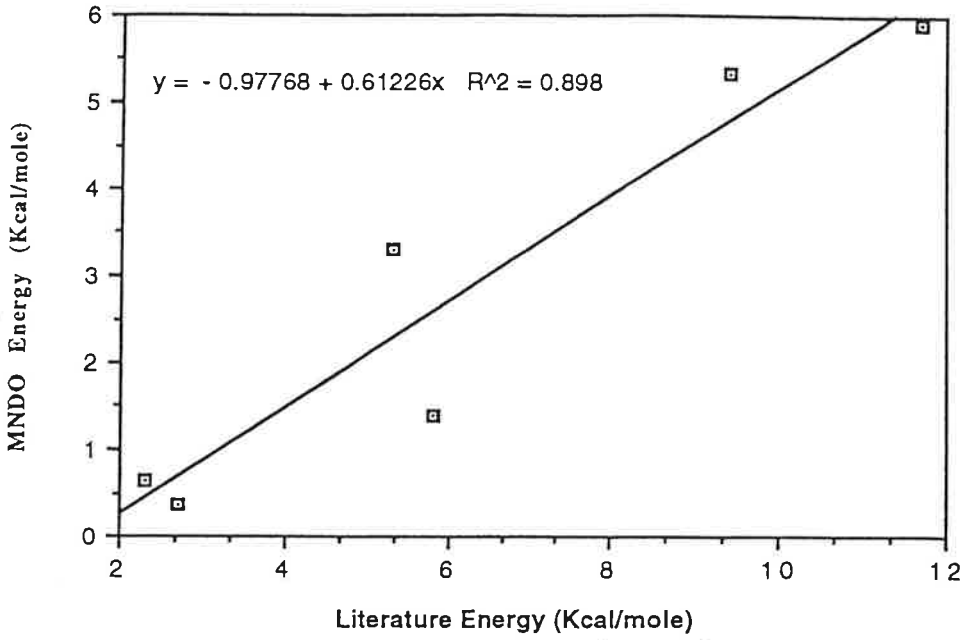

2.2.1.2 Geometry.

Tables 3 and 4 show a comparison of calculated and experimental H-bond angles and XY distances (where X and Y are the two electronegative atoms in a H bond). MM2 (table 3) commits some spectacular errors in XY distances, showing deviations as large as 1 Å. However all these failures involve HF acting as a donor; otherwise the mean error in XY distance is small. MM2 fails to reproduce the linearity of the hydrogen bond in systems in which HF acts as a donor, but seems to do better in the remaining systems. Water-ammonia is also poorly described.

MNDO-PM3 calculations offer a striking improvement in the description of the geometry of the hydrogen-bonding dimers, even for systems in which HF acts as a donor. The linearity of the hydrogen bond is less well described; but the bending mode of the hydrogen bond is very soft. Calculations at the 3-21G* level for both the water and ammonia dimer confirmed the small cost in energy upon the bending of the H-bond. For instance, deviations of even twenty degrees from linearity in the water dimer only affect the overall energy by 0.0912 kcal/mol. In general, the energy cost upon H-bond bending starts to become significant for deviations of forty degrees or more. However, it should be noted that many computations and analyses of experimental data presume linear H-bonds for simplicity, and departures from this ideal may commonplace.

Dimer	XY Dist. (Å)		XHY angle	
	Lit.	MM	Lit.	MM
HF-HF	2.69	3.82	180	146
Water-Water	2.85	2.73	180	176
Ammonia-Ammonia	3.28	3.16	180	176
HF(A)-Water(D)	2.94	2.99	180	170
HF(D)-Water(A)	2.64	3.64	180	135
HF(A)-Ammonia(D)	3.22	3.11	180	179
HF(D)-Ammonia(A)	2.67	3.89	180	132
Water(A)-Ammonia(D)	3.24	2.69	180	128
Water(D)-Ammonia(A)	2.93	3.10	180	168

Table 3. Experimental [9] versus MM2 XY distances and XHY angles.

Dimer	XY Dist. (Å)		XHY (deg)	
	Lit.	PM3	Lit.	PM3
HF-HF	2.69	2.68	180	168
Water-Water	2.85	2.75	180	167
Ammonia-Ammonia	3.28	3.33	180	157
HF(A)-Water(D)	2.94	3.00	180	170
HF(D)-Water(A)	2.64	2.73	180	177
HF(A)-Ammonia(D)	3.22	2.71	180	162
HF(D)-Ammonia(A)	2.67	2.73	180	175
Water(A)-Ammonia(D)	3.24	3.30	180	153
Water(D)-Ammonia(A)	2.93	2.96	180	162

Table 4. Experimental [10] versus MNDO PM3 XY distances and XHY angles. Note that with a few exceptions MNDO PM3 predicts reasonable geometric parameters.

2.2.2 An Intramolecular Hydrogen Bond.

2.2.2.1 Neutral Malonaldehyde.

A. Geometry.

We investigated a system, malonaldehyde, for which a nonlinear intramolecular hydrogen bond is unambiguously established. Tables 5 and 6 show the results of such calculations. Both MM2 and MNDO describe bond distances well, with a single exception in both cases: the H-bond distance, observed to be 1.68 Å. MM2 overestimates the distance by 0.33, while MNDO-PM3 overestimates the distance by only 0.14 Å. Since the bond length is a direct measure of its strength of the bond, MM2 seems to be underestimating such interaction more seriously than MNDO-PM3. This is not surprising from a model that adopts a primarily electrostatic view of chemical bonding. MNDO, making use of its more sophisticated model, is able to introduce more factors (i.e. atomic orbital overlap) into the calculation of the hydrogen bond length and strength.

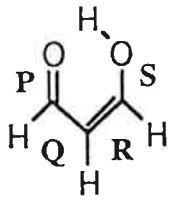

Parameter	Microwave[a]	Mechanics[b]	MNDO-PM3[c]
P	1.234Å	1.208	1.225
Q	1.454	1.473	1.458
R	1.348	1.341	1.356
S	1.320	1.356	1.336
OH	0.969	0.972	0.969
O...H	1.708(1.68)	2.012	1.827
O...O	2.554	2.793	2.644
O-H...O Angle	148°	136	141
P•Q Angle	123	125.7	121.5
Q•R Angle	119.4	122.3	121.8
R•S Angle	124.5	126.8	124.8
S•OH Angle	106.3	110.3	109.3

[a] ref. 11

[b] MM2: This work [c] MNDO-PM3: This work

Table 5 Experimental and theoretical geometric parameters of malonaldehyde. The letters have been assigned according to the structure drawn above. This nomenclature will be used throughout this section on malonaldehyde. Both MM2 and MNDO PM3 agree fairly well with microwave data. The largest deviation occurs with the H-bond length.

Parameter	ab initio[a]	ab initio[b]	ab initio[c]
P	1.233Å	1.248	1.248
Q	1.484	1.452	1.439
R	1.334	1.342	1.362
S	1.365	1.312	1.328
OH	0.998	0.956	0.994
O...H	1.659	1.880	1.694
O...O	2.568	2.676	2.589
O-H...O Angle	149°	139	147
P•Q Angle	122	124.1	123.5
Q•R Angle	119	120.9	119.5
R•S Angle	124.5	126.2	124.5
S•OH Angle	103.9	109.4	105.4

[a] This work: STO-3G. [b] SCF-631G. [c] SCF-631G with MP2 corrections; b and c by ref. 12

Table 6 *Ab initio* geometries of malonaldehyde. MP2 corrections have to be introduced in order to obtain an accurate H-bond distance.

B. Changes attending H-bond formation.

In the previous section we concluded that MNDO PM3 reproduces malonaldehyde's structural features satisfactorily. It is now necessary to check if this model is also able to predicts basic features of H-bonds. Table 7 shows different geometric features and vibrational information for both the exo (non H-bonded) and endo (H-bonded) malonaldehyde. In general we found that MNDO-PM3 gives a very plausible account of the effects upon H-bond formation. The hydroxyl stretching frequency decreases due to the weakening of the formal O-H bond while the torsion and bending modes increase in energy. Furthermore, the O-H bond length is increased by 0.021Å and the O···O distance reduced. Finally, there is also a rearrangement of the primary valence angles of the molecular framework. Upon H-bond formation, malonaldehyde tends to become a more compact ensemble with smaller PQ and RS angles.

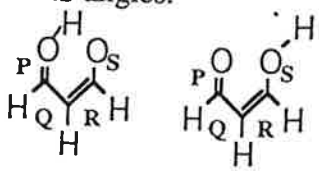

Endo

Exo

Parameter	exo	endo	Cyclohexanol
OH Stretch	3903 cm^{-1}	3647[a]	3895
OH bend	1316	1570[a]	
OH torsion	266	645[a]	196
OH	0.948	0.969[a]	0.948
O...O	2.85	2.644	
P•Q Angle	125.7	121.5	
Q•R Angle	127.7	121.8	
R•S Angle	121.0	124.8	
S•OH Angle	107.0	109.3	106.8

[a] H-bonded.

Table 7 Geometries and vibrational frequencies for the endo (H-bonded) and exo (non H-bonded) malonaldehyde and cyclohexanol. As the table shows most of the characteristic traits of H-bonds are accounted by MNDO PM3.

C. Proton Transfer.

The vast amount of literature dedicated to the proton tranfer in malonaldehyde [13,14,15] is sufficient to justify the use of this molecule to test MNDO-PM3's performance. Figure 5 shows a potential energy surface for the thermal (non-tunneling) proton transfer in malonaldehyde. The procedure followed was rather simple. Each independent variable covered in twelve steps the range of values shown in the plot. A complete energy minimization was done at each point, for a total of 169 points. Obviously, the grid could have been more accurate (i.e increasing the step size of the independent variables over the given ranges of values). However, this would have led to a very long computation.

In the energy map two minima corresponding to equivalent mirror images were found circa -70.5 kcal/mol. Following the minimum energy path from one minimum to the other, the transition state (TS) is allocated between -40 and -50 kcal/mol. Further exploration of the region near the transition state and a transition state search [16] yielded a structure with C_{2v} symmetry, as detailed *ab initio* and semiclassical treatments have shown [17].

Unfortunately, MNDO-PM3 does not perform satisfactorily in describing the energetics of the proton transfer. The energy of activation for the proton transfer, 20-30 kcal/mol) is very large. Literature values range between 10.3 kcal/mol and 4.3 kcal/mol [18,19]. Even with the introduction of tunneling corrections the MNDO-PM3 model would not approach these values, certainly closer to the true energy barrier.

As we saw for the first and second row hydride dimers, while MNDO-PM3 yields reasonable geometries it fails in providing us with accurate energies. This is not very surprising if we remember that PM3 is not parametrized to account for hydrogen bonding and this interaction is therefore an indirect consequence of the specific electronic properties and structure of the molecule. The structures below is a simplified cartoon of the proton transfer process in neutral malonaldehyde.

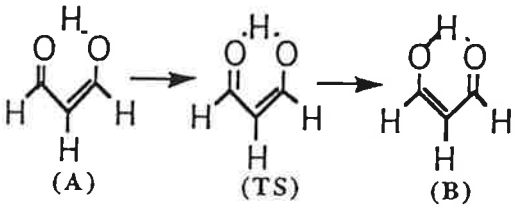

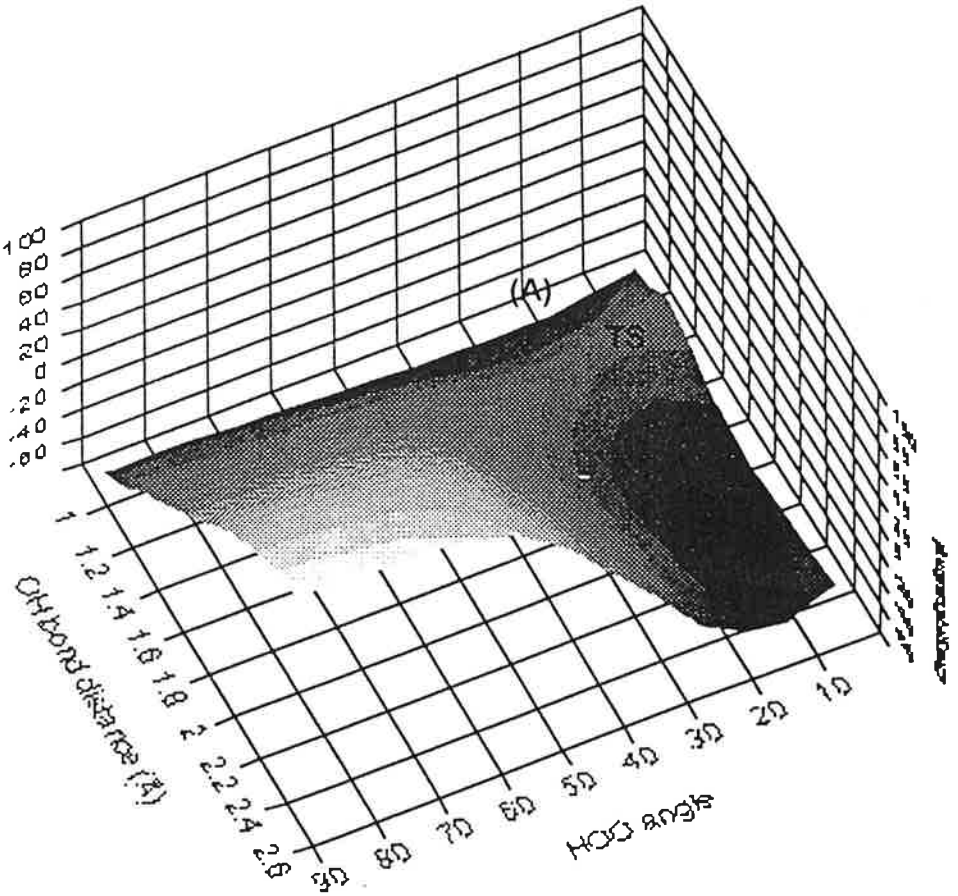

Fig. 5 Potential energy map for the proton transfer in neutral malonaldehyde. The two minima found at -70 kcal/mol correspond to indistinguishable conformations (A and B). According to this surface, the transition state (TS) is somewhere in the region between these two equivalent minima and has an energy between -40 to -50 kcal/mol.

2.2.2.2 Protonated malonaldehyde.

Malonaldehyde could be protonated at two different sites. We have borrowed the following nomenclature from Organic Chemistry to designate the carbonyl-protonated species as the *sym-* diprotonated and the hydroxyl-protonated species as the *gem-* diprotonated.

A. Geometries of the *sym-* and *gem-* diprotonated malonaldehyde.

Table 10 shows the geometric parameters and energies of the lowest-energy *sym-* diprotonated conformer. The energies are referenced to an acidic aqueous environment and show that if the hydronium ion is present protonation at the carbonyl terminus will be favored by around 30 kcal/mol. The bond distances and angles of the *sym-* species suggest that a conventional Lewis picture or even a resonance structure is not satisfactory in describing its structure. For instance, upon protonation the carbonyl double bond elongates while, the CC double bond shrinks. It is also aparent that the hydrogen bond formed upon protonation is also weaker than that found in the neutral species as the elongated O-H and OO distances suggest.

sym-diprotonated species

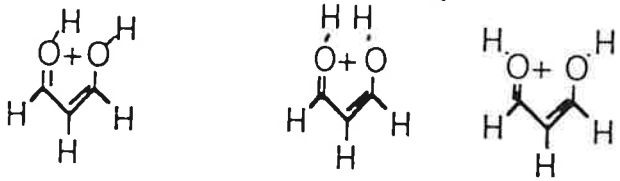

Least-energy Protonated Protonated'

Parameter	Neutral	Protonated
Energy	88.65[b]	52.85
P	1.225	1.292
Q	1.458	1.409
R	1.356	1.356
S	1.336	1.329
OH at S	0.969[a]	0.953
OH at P	-	0.966[a]
O...H	1.827	1.867
O...O	2.64	2.63
O-H...O Angle	141	134.3
P•Q Angle	121.5	125
Q•R Angle	121.8	125
R•S Angle	124.8	116
S•OH Angle	109.3	112
P•OH Angle		113.5

[a] This is part of the H-bond chain.

[b] Kcal/mol; Neutral + H_3O cation; charged species + H_2O neutral.

Table 10 Geometry of the least-energy structure of *sym*-protonated malonaldehyde (MNDO PM3). Parameters have been named according to the nomenclature previously used for malonaldehyde.

Parameter	Neutral	Protonated	Protonated'
Relative energy[b]	88.65	58.73	53.67
P	1.225	1.292	1.308
Q	1.458	1.409	1.393
R	1.356	1.356	1.393
S	1.336	1.329	1.308
OH at S	0.969	0.953	0.954
OH at P	-	0.966[a]	0.954
O...H	1.827	1.867	3.633
O...O	2.644	3.238	2.712
O-H...O Angle	141	125.7	13.0
P•Q Angle	121.5	125	119.9
Q•R Angle	121.8	125	129.0
R•S Angle	124.8	116	119.8
S•OH Angle	109.3[a]	112[a]	111.8
P•OH Angle		113.5	111.8

[a] Part of the H-bond

[b] Kcal/mol; Neutral + H_3O cation; charged species + H_2O neutral.

Table 11 Geometries of the alternative structures of *sym*-protonated malonaldehyde (MNDO-PM3).

Table 11 shows figures corresponding to alternative conformations of the *sym*-diprotonated malonaldehyde. Surprisingly enough, their energies are not much higher than the lowest minimum found, again suggesting the small contribution of H-bonding to the overall energy in even a relatively small system such as malonaldehyde. The conformer labelled protonated' shows a highly symmetric conformation probably owing to an increased amount of delocalization.

Table 12 shows the structural parameters of the *gem*-diprotonated species. Three important features should be emphasized. First, the energy of this conformer is about 30 kcal/mol above the sym-diprotonated. Second, the OH bond length of the hydrogen in the plane of the molecular framework (the OH 'endo') is considerably long and the OO distance somewhat reduced by about 0.96 Å. Third of all, the PQ angle has decreased probably due to a closer proximity of the carbonyl oxygen to the 'endo' hydrogen.

gem- diprotonated malonaldehyde

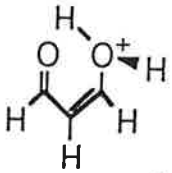

Parameter	Neutral	Protonated	Transition
Energy[b]	88.65	83.89	(90)
P	1.225	1.224	1.238
Q	1.458	1.489	1.482
R	1.356	1.337	1.344
S	1.336	1.436	1.428
OH' "exo"	-	0.970	0.964
OH "endo"	0.969[a]	1.013[a]	1.059
O...H	1.827	1.684	1.417
O...O	2.644	2.550	2.402
O-H...O Angle	141	140.6	151.6
P•Q Angle	121.5	118.2	117.8
Q•R Angle	121.8	123.4	121.3
R•S Angle	124.8	120	117.9
S•OH Angle	109.3[a]	109.3[a]	104.6[a]
S•OH' Angle		106.0	107.5
HCOH'		60.2	58

[a] This is part of the H-bond chain.

[b] Kcal/mol; Neutral + H_3O cation; charged species + H_2O neutral.

Table 12 MNDO PM3 structure of *gem*-diprotonated malonaldehyde. The column labelled 'transition' corresponds to the best guess of the structure of the transition state between both *sym*- and *gem*-diprotonated forms.

B. Proton transfer.

The potential energy surface for the proton transfer in protonated malonaldehyde (fig. 6) is able to provide an explanation for the geometric features found in gem-diprotonated malonaldehyde. In this case, the surface contains two inequivalent minima, separated by 30 kcal/mol. The high energy species is the gem-diprotonated species, also very close to the transition state. In fact, the energy of activation for going from the *gem*- to the *sym*- structure is only about 6 kcal/mol. The transition state is very close in both energy and geometry to the relative minimum corresponding to *gem*- diprotonated

malonaldehyde in agreement with Hammond's postulate for very exothermic reactions. The anomalously elongated bond and other features found in the minimum energy conformation for gem-diprotonated malonaldehyde is just a direct consequence of the energy difference between both protonated species.

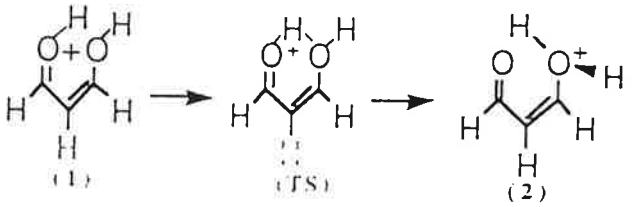

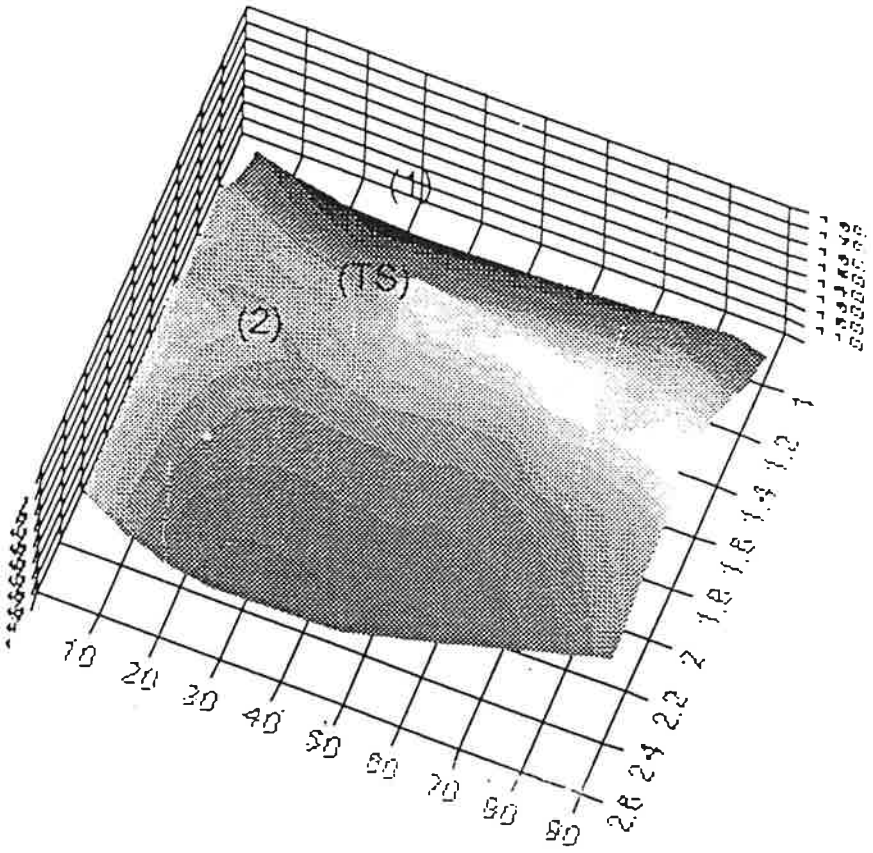

Fig. 6 Potential energy map of the proton transfer in charged malonaldehyde. In this case, the potential energy wells are asymmetrical, the carbonyl-protonated species (1) being favored by about 30 kcal/mol over the hydroxyl-protonated (B) species.

Figure 7 is a three-dimensional plot of the energy of this proton transfer as a function of OH bond distance and HOCH torsion angle (where the HO is the 'exo' hydrogen in the nomenclature previously used). This map provides useful hints of the dynamics of the proton transfer. In going from the *gem-* to the *sym-* conformation, the rearrangement of the OHCH torsion angle occurs very rapidly and the rest of the process is practically limited to a bond elongation that transfers the proton from one oxygen to the other. In summary, geometric rearrangement of malonaldehyde is very fast and limited to

an appreciable change in the HOCH torsion angle and minor structural variations of the overall molecular framework.

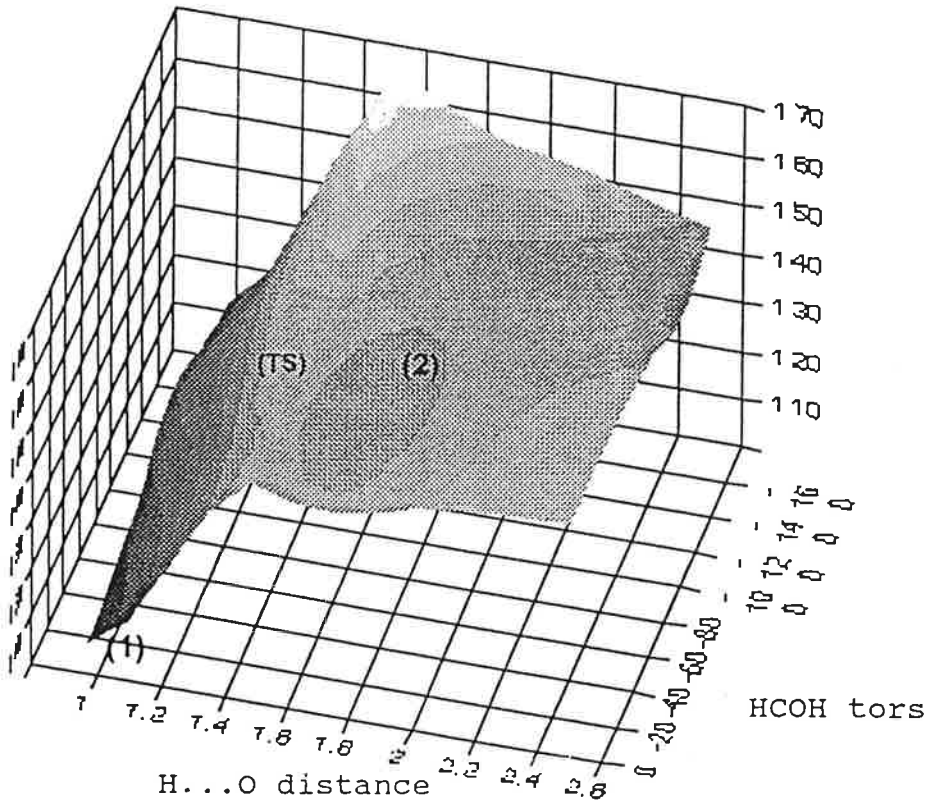

Fig. 7 Potential energy map for the proton transfer of protonated malonaldehyde. As the plot shows, significant deviations from planarity come about after the OH bond has elongated near the dissociation value.

2.2.3 Cyclohexanol.

2.2.3.1. Neutral cyclohexanol.

Before embarking on a study of fused-tricyclic triols, we addressed simpler ring alcohols. In cyclohexanol (fig. 8), one would not expect any type of stabilising effect across the ring. The MM2 force field calculation shows that the [0] conformer (where the brackedted [angle] is the HOCH dihedral angle) is more stable than the [180] species, but less stable than the [60] species as *ab initio* calculations at the 3-21G* level show (see ref. 20 and table 13). MNDO PM3 calculations show the same relative order for the [0] and [60] conformers but predicts the [180] species to be the most stable by about 2 kcal/mole. The MNDO program is considering and clearly overestimating an interaction of the hydroxyl group with the ring, something worthwhile remembering in future studies of rings.

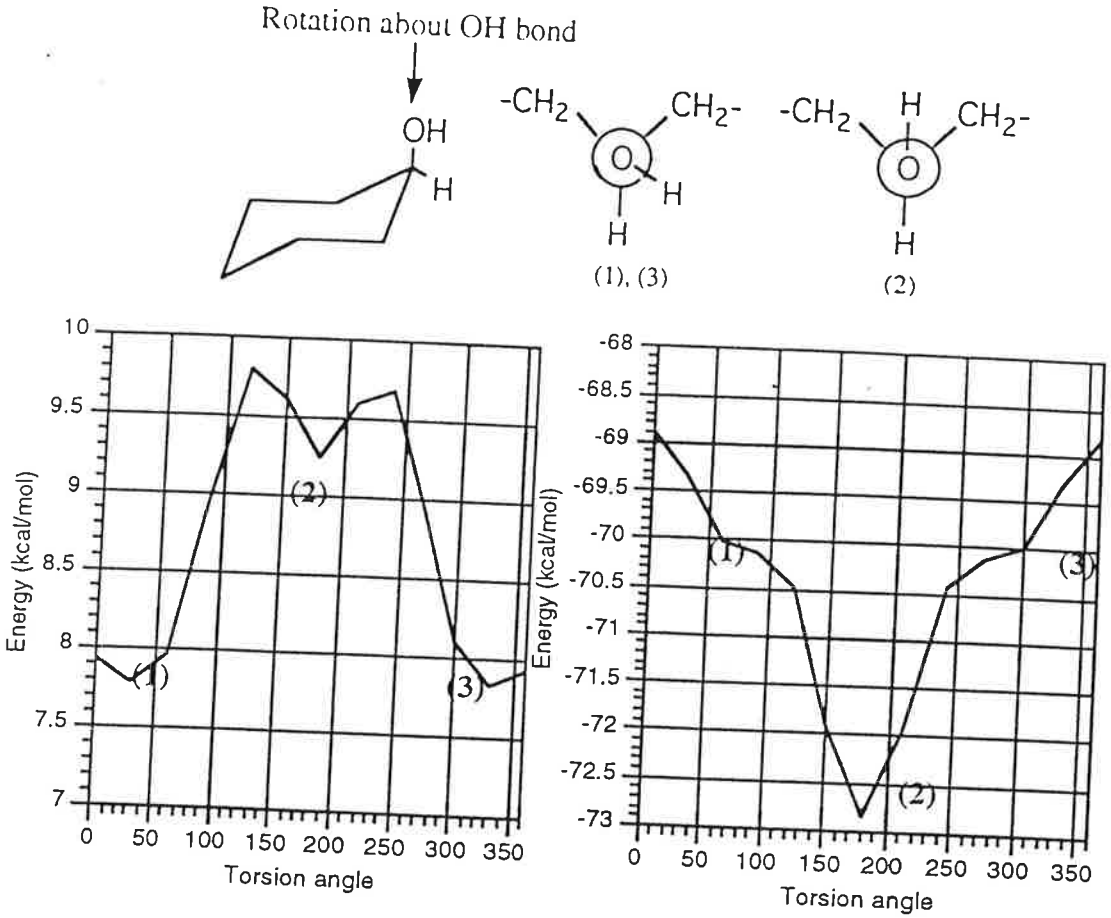

Fig 8 MM2 (left) and MNDO PM3 (right) reaction coordinate plots for the 360-fold rotation of the OH group in cyclohexanol. Structures of the numbered critical points have been provided above. Vibrational analysis of structures (1) and (3) showed that they are shallow minima yet this feature is not apparent from the map here presented.

Relative E kcal/mol	Molecular Mechanics[a]	MNDO-PM3[b]	*ab initio* (321*)[c]
60°	0	0	0
180°	1.47	-2.82	1.85

a,b,c this work.

Table 13 MM2, MNDO PM3 and *ab initio* energies for the [60] and [180] rotational conformers of cyclohexanol. The [0] and [120] conformers are maxima between the [60] and [180] rotamers. As the figures show, MNDO PM3 clearly prefers the [180] conformation.

The only difference between MM2 and MNDO PM3 results are in the COH angles, which MNDO does not change appreciably when the hydrogen goes over the ring. Currently, there is no solid explanation of this effect but it could be very well interpreted as a direct consequence of the approximate character and unpredictable lack of reliability of this semiempirical model.

2.2.3.2 Charged Cyclohexanol.

The structures and relative energies of different rotational conformers of charged cyclohexanol have been provided below.

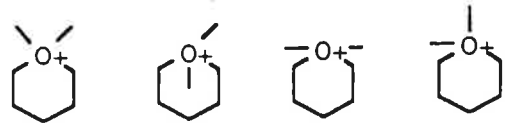

60,-60 180,-60 120,-120 0,-120

Relative energy in kcal/mole			
60,-60	180,-60	120,-120	0,-120
3.06	0	1.34	

Table 14 Low Energy Conformations of Protonated Cyclohexanol (MNDO-PM3).

Again, MNDO's bias seen before is repeated for this structure. Only one striking structrural difference between the neutral and charged cyclohexanol: the CO bond length, which increases by about 0.1 Å upon protonation. This result has been corroborated recently by ab initio calculations at the STO-3G and 3-21G* level.

2.2.4 Bicyclic Diols.

Figure 9 shows the convention used to name the different conformer for the bicyclic species.

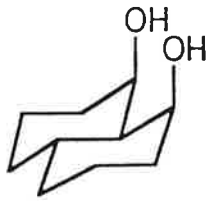

Bicyclo [1.6] decan-2,10-diol diaxial isomer

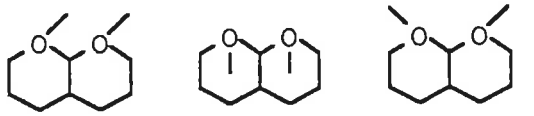

L=+60 R=-60 L=180 L=180 L=-60 R=-60

Fig. 9 Above, the generic structure of the bicyclic system, with both hydroxyl groups in the axial position. Below several rotational conformers of this diaxial species. The adopted convention for signs goes as follows: torsion angles locating hydroxyl hydrogens are measured from equatorial hydrogens at left and right; 'handed' convention for signs: +torsion angle at left = clockwise (left hand rule), +torsion angle at right = anticlockwise (right hand rule).

2.2.4.1. Neutral bicyclic.

Tables 15 and 16 show again MNDO's prejudice towards over-the-ring conformers. No such prejudice was observed at an STO-3G *ab initio* level. However, both MNDO and *ab initio* have a common feature, namely that the torsion angle for the hydrogen involved in H-bonding is swung toward O-H colinearity.

Energy (kcal/mol)	Left Angle	Right Angle	Note
0.0	89	-62	H-bond
+6.0	-116	-75.8	No H-bond
0.9	160.1	-53.6	R
-1.05	174.4	172.4	2R
-2.5	-166.5	-79.6	R & H

Table 15 MNDO PM3 energies for different rotamers of neutral bicyclic. 'R' means an OH is over a ring. MNDO is biased toward placing OH over the ring, as we saw in cyclohexanol.

Energy (kcal/mol)	Left Angle (L)	Right Angle (R)	Note
0.0	78.3	-54.4	H-bond
0.85	164.8	-71.45	R

Table 16 *Ab initio* STO-3G energies for different rotamers of neutral bicyclic.

In an attempt to treat MNDO's pathology towards ring systems, several rigid reaction coordinate searches were performed with different starting geometries. Figures 10 and 11 show that if the starting geometries have no hydrogens over the ring, MNDO mimicks the *ab initio* results. However, by starting with a structure with hydrogens over the ring, the bias towards the over the ring conformations appears once more (fig. 11). This result suggests that those conformations with no hydrogens over the rings could be treated separately from those with hydrogens over the rings.

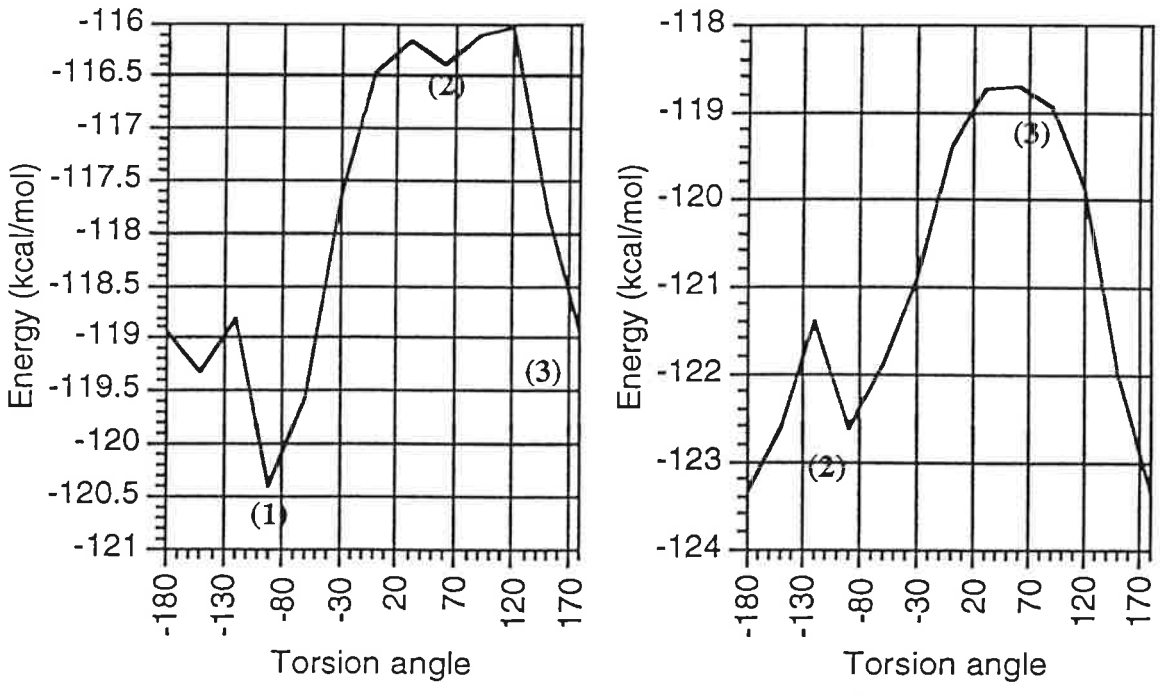

Figs. 10 and 11 MNDO PM3 profiles for the rigid rotation of one hydroxyl group over its CO bond. The starting geometry were the optimized -60/60 and the 180/180 cnformations for the left and right plots respectively. Note that MNDO's bias disappears when full optimization is performed with a rotamer with no hydrogens over the cyclohexanol ring.

2.2.4.2 Charged bicyclic.

A. Geometries.

Tables 16-20 offer a brief summary of the main structural traits of the low-energy conformations of bicyclic diols. These systems repeat some of the structural features already seen in simpler systems including MNDO's misbehavior with ring systems. For instance, OH bonds involved in H-bonding are extended from 0.95 to 0.99 Å and are twisted toward colinearity. CO bonds also elongate to 1.52 Å upon protonation.

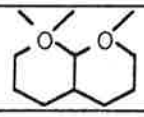	NAME: -60, +60, -60 Relative Energy +3.3 H···O = 1.853		
Torsions	-64.4	+66.2	-103.7
OH lengths	0.947	1.000	0.981
O···O	2.701	OH···O	140.6
COH angles	106.7	105.0	105.2
CO lengths	1.420		1.414

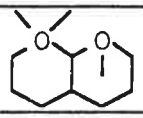	NAME: -60, +60, +180 Relative Energy +3.3 H···O = 1.693		
Torsions	-36.7	+83.5	-148.7
OH lengths	0.964	0.998	0.955
O···O	2.593	OH···O	147.8
COH angles	107.0	107.2	107.4
CO lengths	1.521		1.427

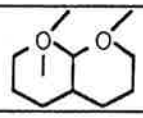	NAME: 60, 180, -60 Relative Energy +0.9 H···O = 1.712		
Torsions	79.1	+197.2	-65.2
OH lengths	0.992	0.979	0.948
O···O	2.567	OH···O	141.9
COH angles	107.0	105.7	107.8
CO lengths	1.510		1.428

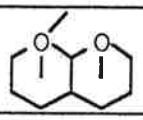	NAME: 60, 180, 180 Relative Energy +0.0 H···O = 1.703		
Torsions	84.8	+203.1	-147.2
OH lengths	0.997	0.977	0.955
O···O	2.596	OH···O	147.0
COH angles	107.2	106.2	108.0
CO lengths	1.509		1.426

Tables 16-20 MNDO-PM3 low-energy conformations of protonated bicyclic diols. Not only MNDO's bias towards ring systems is present but also some important structural features of H-bonding.

B. Proton transfer.

Figure 12 is the potential energy surface for the proton transfer in the charged bicyclic system with a hydrogen bond and all hydroxyl hydrogens out of the ring.

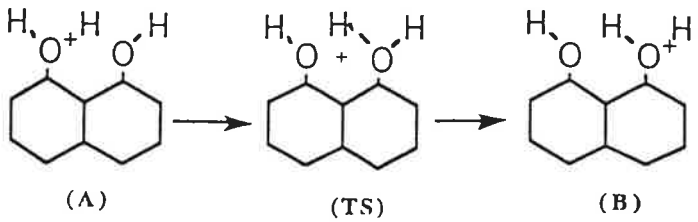

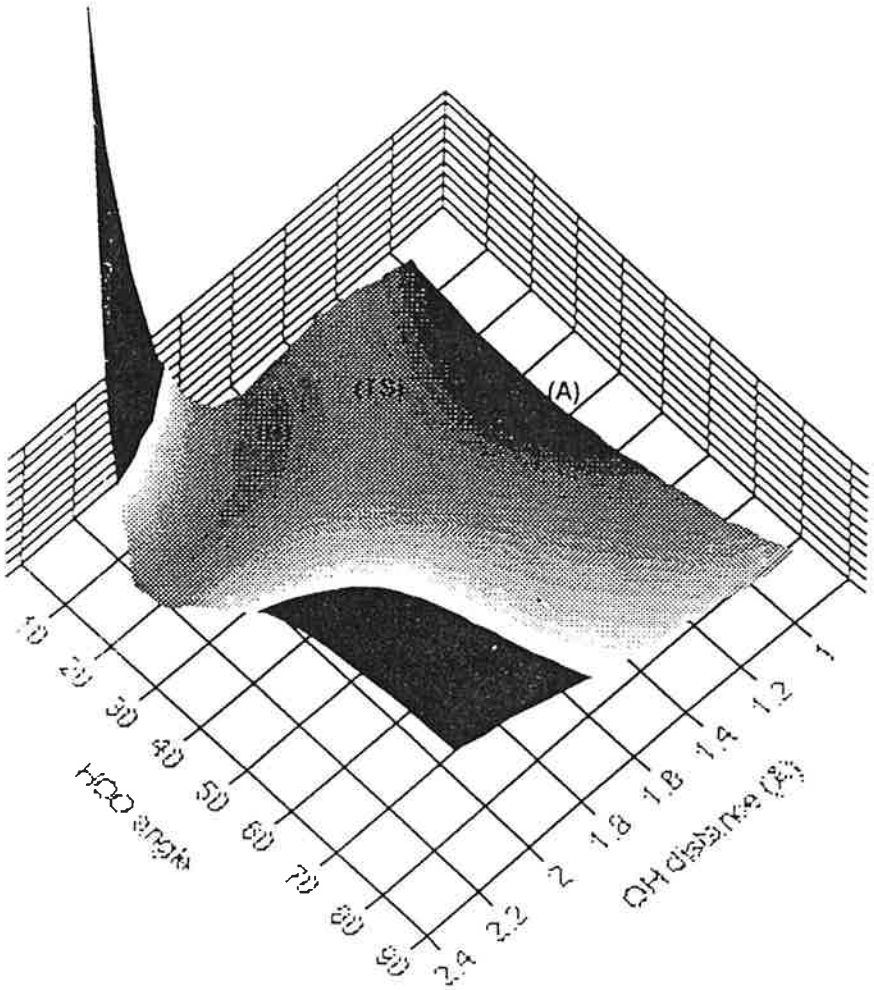

Fig. 12 Potential energy surface for the proton transfer of the -60/60,-60 rotamer.

The surface contains two equivalent minima as well as a transition state circa 20 kcal/mol over these minima. The minimum energy path between both energy wells suggests that minor structural rearrangements take place during the proton transfer. Initially, the OH bond elongates near the dissociation limit and then angular and radial rearrangements take place altogether in the region near the transition state in order to complete the proton transfer.

2.2.5 Tricyclic triols.

The study of tricyclic triols is its early stages. A few calculations using MM2 and MNDO PM3 have been performed. MM2 predicts substantial H-bonding stabilization with an H-bond distance between 1.8 and 2.0 Å and a O···O distance between 2.6 and 2.7 Å. The OH···O angle is in the range of 130-135 degrees, and torsion angles are either 45 or 65 degrees, the larger torsion angles accomodating the hydrogen bond.

MNDO PM3 calculations yield a O···O distance around 2.6 Å, a H-bond distance at 1.8 and the OH···O angle near 145. Torsion angles are somewhat larger than those predicted by MM2. They can be near 60 or 80 degrees depending on whether the hydrogen is participating in a H-bond in which case the torsion angle approaches the larger value.

This preliminary modeling of polycyclic polyols show that the main traits observed in the smaller systems will persist for longer chains constructed of fused 6-membered rings.

2.6 Conclusions.

- General Utility of Modeling Methods for the Study of Hydrogen Bonding: Rough but Pleasing

- **Malonaldehyde**: the H bond is nonlinear but well established. MNDO reflects observed changes in the OH stretching and bending frequencies and in the bond length associated with H-bonding. The barrier to thermal (not tunneling) proton transfer is substantial, requiring an extension of the OH bond by >25%. MNDO overestimates the proton transfer barrier (>35 kcal/mol).

- Protonation of malonaldehyde would occur at the carbonyl. The *gem*- diprotonated species rearranges to the *sym*- diprotonated species, over a small barrier (*ca.* 6 kcal/mol). The transition state closely resembles the unstable *gem*- diprotonated species, in accord with Hammond's postulate.

- $H_{eq}COH$ torsion in axial **cyclohexanol** is very easy. MNDO-PM3 unrealistically favors the *endo* orientation of the OH (in which it hovers over the ring) but otherwise gives a plausible account of the COH environment.

- Diaxial **bicyclic diols** are stabilized by a hydrogen bond; the picture is clouded by MNDO's bias toward the *endo* orientation of the OH bond. Despite the MNDO prejudice, we can see that in all orientations H-bonding alters the $H_{eq}COH$ torsion angle, bringing the OH···O fragment closer to the colinearity favored by hydrogen bonds.

- Protonation of the bicyclic diols produces several species closely comparable in energy. The structure with no OH bonds rotated over the ring suffers MNDO's bias, and shows extension of the CO[+] bond upon protonation. The barrier to proton transfer is estimated by PM3 to be greater than that found in charged malonaldehyde, although we judge that little structural reorganization is required as transfer takes place.

- Preliminary modeling of fused tricyclic triols suggests that the energetic and structural features found in diols will persist. Proton transfer occurs by displacement-replacement steps with very little structural reorganization.

- Even more tentative modeling hints that the geometry of fused-ring scaffolding structures for polyalcohols is most favorable for all ringsizes = 6. The favored quasi-rigid structure orients the OH groups so that only low-cost torsions need accompany proton transfer.

2.7 Future Work.

It is clear from this work that the project is still in its very early stages. MNDO PM3 can be very useful at times but it can also fail unpredictably. Perhaps, the weakest part of this project has been the lack of experimental data to support our assumptions and conclusions about many of the structural features found for polycyclic polyols. However, experimental data of this sort is very scarce in the literature. Prof. Glen McGarvey, here at the UVA Chemistry Department, has an NMR study of the structure of polyol systems. Unfortunately, these NMR spectra show no conclusive information on the hydrogen bonding in those systems. Chemical shifts characteristic of H-bonded hydrogens are very ambiguous, if not absent.

On the other hand, *ab initio* data on, for example, the potential energy surface for the proton transfer in bicyclic would be of great help. At this point in time, calculations of this sort could be very lengthy. Fortunately, the next version of the software package SPARTAN, distributed by Wavefunction Inc., will allow the generation of potential energy grids at the semiempirical and even *ab initio* level; this will surely estimulate a more precise study of hydroxyl chains.

So far, semiempirical models have let us determine the broad features of proton transfer in hydroxyl chains. Probably, it is time now to use a higher level of theory and computation in order to obtain a more insightful picture of the process.

3. A Remark on the Ionic vs Covalent Views of the Hydrogen Bond.

Given these general features, a donor-acceptor picture of H-bonds is a very attractive one, though not totally justified. According to this model, in a H-bond the H1s orbital is the electron acceptor while the electronegative atom utilize more directional p orbitals. The linear hydrogen bond is a reflection of the fact that a highly anisotropic orbital, namely a p orbital, takes part in the interaction [22]. The aforementioned shift of twenty degrees in the dihedral angle of the non H-bonded hydrogen could be accounted using the model given above. Dihedral destabilisation is overcome by the tendency of the hydroxyl groups to hydrogen-bond as linearly as possible. Hydrogen bonds will try to be as linear as the geometric and energetic constraints of the molecule allow.

4. Acknowledgements.

My most sincere thanks to my research advisor, Dr. Carl Trindle, for his guidance and infinite patience during the course of the project. I would also like to thank Dr. Michael Sabat for helping me with the computing facilities at the Chemistry Department.

Finally, I wish to express my gratitude to Dr. Glenn McGarvey for suggesting the problem and the model system and also to his posdoctoral student Grant Spoors for providing us with NMR data on the polyol chain.

References.

[1] W. M. Latimer and W. H. Rodebush, J. Am. Chem. Soc., **42**, 1419 (1920)

[2, 3] Schuster, P. et al. Top. Curr. Chemistry. 1984, **120**, 1: 36
For an excellent review of the experimental techniques currently used in structural chemistry see, P. J. Wheatley's *The Determination of Molecular Structure*, Dover Publications Inc., New York, 1968.

[4, 6, 8, 9, 10] Kollman, P.A. et al. JACS, **97(5)**, 955 (1975).

[5] Dyke, Th. R., et al. Top. Curr. Chemistry. 1984, **120**, 1: 110.

[11] E. B. Wilson and Z. Smith, Accts. Chem. Res. 1987 **20**, 257

[12] M. Frisch, H. F. Schaefer III, J.S. Binkley, J. Chem Phys. 1985, **82**, 4194

[13] Seliskar C. J. , Hoffmann, R.E., Journal of Molecular Spectroscopy, **96**, 146-155 (1982)

[14] Shida, N. et al., Journal of Chemical Physics, 1989, **91**, 4061

[15] Bosch, Enric et al., Chemical Physics, **159** (1992), 99-107

[16] Dewar, J.S. et al., Journal of the Chemical Society, Faraday Transactions II, **3**, 227 (1984)

[17,18] Carrington, J. and Miller, W., Journal of Chemical Physics **84(8)**, 1986, 4364

[19] Frisch et al., J. of Chemical Physics, **82**, 4194 (1985)

[20] Palke, W. E. et al., J. Phys. Chem. 1988, **92**, 3046-3048

[21] Grant Spoors, personal communication.

[22] Klemperer et al., J. of Chem. Phys., **67**, 5177 (1977)